American Journal of Science and Technology
2016; 3(1): 1-11
Published online January 6, 2016 (http://www.aascit.org/journal/ajst)
ISSN: 2375-3846

American Association for Science and Technology

A Rating Model for Air Cooled Condensers Using Pure and Blend Refrigerants

Ali Hussain Tarrad[1], Ayad Khudhair Al-Nadawi[2]

[1]Private Consultant Engineer/Mechanical Engineering, Copenhagen, Denmark
[2]Department of Machinery and Equipment, Technical Institute/Al-Anbar, Middle Technical University, Iraq

Email address
dr.alitarrad@yahoo.com (A. H. Tarrad), ayadkhudhair@yahoo.com (A. K. Al-Nadawi)

Citation
Ali Hussain Tarrad, Ayad Khudhair Al-Nadawi. A Rating Model for Air Cooled Condensers Using Pure and Blend Refrigerants. *American Journal of Science and Technology.* Vol. 3, No. 1, 2016, pp. 1-11.

Keywords
Air Cooled,
Heat Exchanger,
Modeling,
Refrigerant Alternatives,
Zeotropic Blends

Received: December 02, 2015
Revised: December 14, 2015
Accepted: December 16, 2015

Abstract
The present research represents a mathematical rating model applied for an air cooled louvered finned tube condenser. The energy and continuity equations at the steady state conditions together with available correlations in the open literature were implemented in the present model. The steady state experimental data of a window type (2) ton of refrigeration air conditioning unit was used to build a tube by tube model to investigate the evaporator performance. The refrigerants selected for this object were R22 and the zeotropic blends R407C and R407A refrigerants. The validation of the present model for pure and mixtures showed good agreement between experimental and those predicted values. The predicted duty when circulating R22 and R407C refrigerants exhibited under prediction behavior scatter by (-5%) and (-4%) respectively. On the contrary, R407A simulation results revealed over prediction by a maximum of (+1.7%). The simulation showed that when circulating R22 in the unit, maximum discrepancy between predicted and measured air temperature at entry to the condenser ranges between (+21.3% and –7.8%). When R407C refrigerant was circulated, the maximum discrepancy in air temperature simulation was in the range (-11% and 11.6%). R407A revealed over predicted results, the maximum discrepancy was within (24.3%).

1. Introduction

The modeling of finned tube condenser is quite a difficult task. This is because of the complexity of the two-phase flow and heat exchanged process between the refrigerant and air stream. There are many postulated techniques and models that have been built to deal with change of phase phenomenon. Some of these models are available as commercial software or codes with a lack of technical information related to the methodology and design limitations.

Ellison et al. (1981) [1], presented a computer model for an air-cooled refrigerants condenser. The model relies on a tube-by-tube computational approach calculating the thermal and fluid flow performance of each tube in the heat exchanger individually using the local temperature and heat transfer coefficients. The verification of the model with R22 as a refrigerant revealed that the calculated quantity agrees well with the experimental condenser performance parameter. *Domanski* and *Didion (1983) [2]*, focused on the mathematical modeling and prediction of performance of the vapour compression refrigeration system under steady state conditions. The evaporator and condenser models were developed on tube-by-tube technique which the problems of heat exchanger reduce to tube problem. A comparison of computer results against laboratory test data showed that the maximum discrepancy was (3.4%) for cooling capacity.

Kempiak and *Crawford (1991) [3]*, developed a model for a mobile air conditioning condenser. This model was developed to study a replacement of R12 a refrigerant commonly used in mobile air conditioning by R134a which required numerous changes in equipment design to be as reliable and efficiency as R12. In this study, the condenser can be modeled as three sections; desuperheating, condensing, and sub-cooling. The overall heat transfer coefficient and friction factor of each section can be determined. The energy balance model determined the fraction of each section with condenser within (∓ 5). Calculated pressure drop results were within error as high as (-22%), but the majority of the data was within (∓10).

Bensafi and *Borg (1997) [4]*, developed a computational model for detailed design of finned-tube heat exchanger. Coils are discretized into tube element which is based on tube-by-tube technique. Comparison with experimental data of water, R22, R134a, and R407C showed discrepancies of (∓5%) on the coil duty. Also, the comparison results showed larger duties obtained for R407C when compared to R22 for evaporator and condenser. *Sadler (2000) [5]*, presented a condenser model and integrated into air conditioning system. A base condenser model was chosen and design conditions were established at 35 $^\circ C$ and using R22 as a refrigerant. The operating parameter sub-cool and air face velocity were examined over a wide range of ambient condition to determine their effects on the *C. O. P.* It was concluded that the tube diameter and tube circuiting could not be considered separately because both affect the refrigerant pressure drop.

Wright (2000) [6] presented a condenser model to predict the coil performance and optimization using R410A, as a working fluid. The results of this study were compared with the results presented by Sadler [5] to show the difference between R22 and R410A. It is expected that the best performing condenser configurations investigated for R410A air conditioning system would require fewer tube per circuit than the best condenser configurations investigated for R22 in systems similar to those investigated in this work. *Tarrad* and *Khudor (2015) [7]* have presented quite a simple and adaptable correlation for the air side heat transfer coefficient based on a dimensional analysis. They concluded that their correlation predicts the heat duty and overall heat transfer coefficient of the case study heat exchangers with total mean absolute errors of (13%) and (10%) respectively. More recently, *Tarrad* and *Altameemi (2015) [8]* implemented the step by step numerical technique along the steam flow direction to rate a vertical orientation single pass two tube rows heat exchanger. The simulated data showed excellent agreement with the measured rating parameters regarding the heat exchanger load duty and exit air cooling temperature. The respective discrepancy for the heat duty was within (12) % and (-5) % and the exit air temperature was underestimated by (5) %.

In the present work a simulation model was built for rating objectives of finned tube condenser used in air conditioning unit using alternative refrigerants to R22. The model represents an accurate technical tool for the thermal and hydrodynamic prediction of a suitable alternative that may be implemented in an existing refrigeration unit without a major modification. It depends on the technique of performing a step by step solution following the flow of refrigerant in a tube by tube procedure. The model is capable to handle the prediction of the different parameters describing the heat transfer process for both sides of the evaporator. The most interesting and attractive result of the present model is its capability to reveal the distribution map of the operating conditions such as pressure, vapor quality, air temperature and heat duty throughout heat exchanger tube bank. Further, it has the ability to investigate the suitability of tube circuiting for a given heat exchanger arrangement and available surface area. In this category, the model can examine existing tube circuiting for the refrigerant side where it is capable to handle the condensation load of the flowing refrigerant.

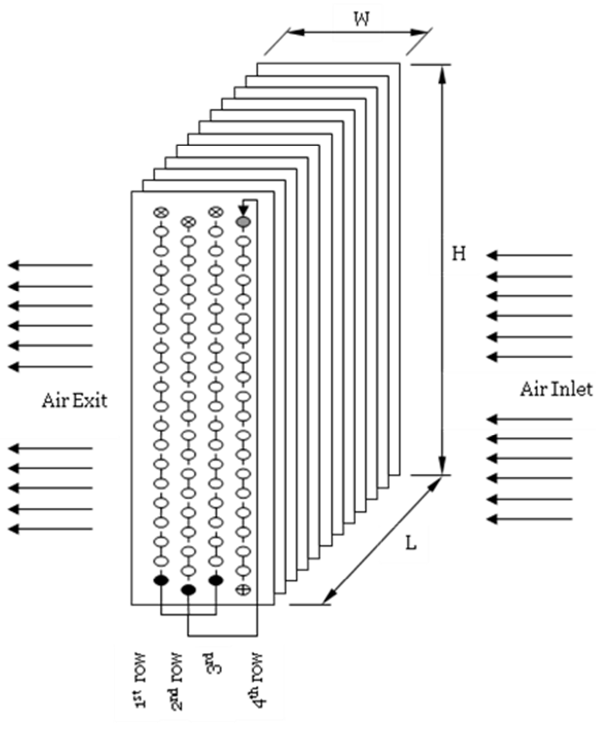

Figure 1. *The Tube Circuiting of the Condenser, Al-Nadawi [9].*

2. Model Background

2.1. Condenser Structure

The condenser possesses three circuits in three rows and these circuits are brought together to form the fourth row, Fig. 1. This mode will triple the mass flow rate and increase the heat transfer coefficient. Table 1 shows the overall physical dimensions of the heat exchangers. It is of the interrupted louvered fin type, *Al-Nadawi (2010) [9]*. The interrupted fin is very widely accepted method of increasing the heat transfer coefficient, as this type involves creating more turbulent mixing on the air side of heat exchangers. It is clear that the air temperature at the first three rows is unknown, so the outlet temperature of the first row is used to determine the inlet air temperature of this row and then the mean value of this temperature is taken and used as the outlet temperature of the row number two and the simulation progresses until it reaches the fourth row.

Table 1. *The characteristic physical dimensions of the condenser, Al-Nadawi [9].*

Parameter	Value
Tube Length (mm)	560
Dimension (L×W×H) (mm)	560×45×400
No. of Circuits	3
No. of Rows	4
Tube outside diameter (mm)	7.9337
Tube inside diameter (mm)	6.22
Tube metal	Copper
Transverse tube pitch (mm)	18.65
Longitudinal tube pitch (mm)	18.65
Fin thickness (mm)	0.137
Fin pitch (mm)	1.5
Total No. of fin	342
Fin metal	Aluminum
Area of heat exchanger (m^2)	10.75
Area of fin (m^2)	9.61
Area of tube (m^2)	1.145

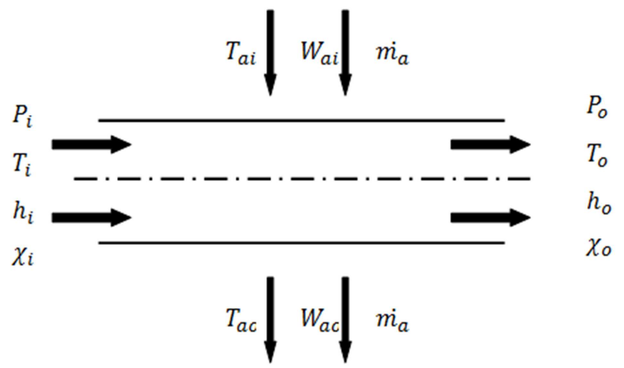

Figure 2. *Control Volume of an Individual Tube, [9].*

2.2. Model Strategy

The tube-by-tube method is implemented to build up CONTBT program and evaluates the performance of a single finned tube condenser. This method reduces the general finned coil to a single tube problem classified as steady state-distributed parameter model [1], Fig. 2. In a forward technique, the selection of tube for performance evaluation is at the same direction as the refrigerant or air flow and the outputs are the outlet air and refrigerant parameters. The backward technique establishes its performance at the opposite direction of the refrigerant or air flow. The configuration of heat exchanger circuit will control the way that may be used to model the heat exchangers. The refrigerant which comes from the compressor is spilt into three branches and each branch enters one row. So, the entrance of refrigerant falls in the far side of the air entrance. This circuit arrangement imposes the backward technique in the air side. Thus, by using the outlet air temperature of the condenser together with the inlet refrigerant parameters, the model performance evaluation is established.

In the refrigerant side, the refrigerant travels in the tube regardless of the position wherever the entrance of the refrigerant to the circuit is. It should be noted that the pressure at the exit of each tube is unknown thus this pressure in the first tube is assumed. The assumed value is used to find the refrigerant parameter such as the thermo physical properties of refrigerant which will be used to find the pressure drop of the tube then this pressure drop is compared with the assumed pressure drop. If they do not agree within the specified tolerance, the new value of exit pressure will be used to repeat the calculation process until converge is achieved. After the convergence has been achieved, the exit pressure is used as inlet pressure to the next tube and the same procedure is repeated until the whole heat exchanger is simulated. To find the quality of the refrigerant, it is assumed that heat flux is constant due to a small change of temperature of air during operation and hence the quality varies linearly through the heat exchanger, *Kempiak* and *Crawford (1991) [3]*.

2.3. Continuity Equation

The conversation of mass principle of control volume can be expressed as:

$$\frac{d}{dt}\int_{CV}\rho dV + \int_{CS}\rho(\vec{V}.\vec{n})dA = 0 \tag{1}$$

Splitting the surface integral in the above equation into two parts-one for the outgoing flow stream (positive) and one for the incoming streams (negative) then the general conversation of mass relation can be expressed as:

$$\frac{d}{dt}\int_{CV}\rho dV + \sum_{out}\rho V_n dA - \sum_{in}\rho V_n dA = 0 \tag{2}$$

The parameter (A) represents the cross sectional area of the flow conduit. Equation (2) can be expressed as

$$\frac{d}{dt}\int_{CV}\rho dV = \sum_{in}\dot{m} - \sum_{out}\dot{m} \tag{3}$$

or

$$\frac{dm_{CV}}{dt} = \sum_{in}\dot{m} - \sum_{out}\dot{m} \tag{4}$$

For steady flow process through the heat exchangers so equation (4) would be:

$$\sum_{in}\dot{m} = \sum_{out}\dot{m} \tag{5}$$

2.4. Energy Equation

The energy equation for a fixed control volume can be expressed by:

$$\dot{Q}_{net,in} + \dot{W}_{shaft,net\ in} = \frac{d}{dt}\int_{CV} e\rho d\mho + \sum_{out}\dot{m}\left(h+\frac{V^2}{2}+gz\right) - \sum_{in}\dot{m}\left(h+\frac{V^2}{2}+gz\right) \quad (6)$$

For steady state flow, $\frac{d}{dt}\int_{CV} e\rho d\mho = 0$, and typically heat exchangers involve no work interaction and negligible kinetic and potential energy change $\left(\frac{V^2}{2} = gz = 0\right)$. The term $e = u + \frac{V^2}{2} + gz$, is the total energy per unit mass.

Rearranging and substituting in (6),

$$\dot{Q}_{net,in} = \sum_{out}\dot{m}\,h - \sum_{in}\dot{m}\,h \quad (7)$$

Then the final expressions of general formulae for the mass conservation and energy balance, (5) and (6) respectively were implemented in the present rating model.

3. Refrigerant Side Heat Transfer Coefficient

3.1. Single Phase Forced Convection

Single phase forced convection takes place at the condenser inlet where the superheated vapor is being cooled and at the exit of the condenser where the liquid is being sub-cooled. The heat transfer coefficient of the single phase (sub-cooled and desuperheated) region for all the refrigerants used can be calculated by the correlation of Kay & London cited in *Stewart (2003) [10]* as:

$$St\,Pr^{2/3} = a_{st}\,Re_{Di}^{b_{st}} \quad (8)$$

Where the coefficients a_{st} and b_{st} are:
Laminar $Re_{Di} < 3500$ $a_{st} = 1.10647$ $b_{st} = -0.78992$
Transition $3500 \le Re_{Di} \le 6000$ $a_{st} = 3.5194 \times 10^{-7}$ $b_{st} = 1.03804$
Turbulent $Re_{Di} > 6000$ $a_{st} = 0.2243$ $b_{st} = -0.385$
And

$$St = \frac{Nu_D}{Re_{Di}Pr} = \frac{\bar{\alpha}}{GCp} \quad (9)$$

3.2. Condensation Heat Transfer Coefficient

For predicting the heat transfer coefficient during condensation, Shah cited in *Thome (2008) [11]* proposed an enhancement model that enhances the single-phase heat transfer coefficient of the flowing liquid by a two-phase enhancement factor. The model has a mean deviation of about (15.4%) and compared with many pure fluids such as water, R11, R12, R22, R113, methanol, ethanol, benzene, toluene and trichloroethylene. Further, it has been verified for many different tube sizes and tube orientations.

For a given quality:

$$\alpha = \alpha_l\left\{(1-\chi)^{0.8} + \frac{3.8\,\chi^{0.76}(1-\chi)^{0.04}}{Pr^{0.38}}\right\} \quad (10)$$

where,
α_l= Single-phase liquid heat transfer coefficient by Dittus-Bolter correlation.

The Silver-Bell-Ghaly cited in *Thome (2008) [11]*, method is used to predict the heat transfer coefficient of R407C and R407A. This method includes the effect of mass transfer resistance. The condensing heat transfer coefficient for the mixture is expressed as:

$$\frac{1}{\alpha} = \frac{1}{\alpha(x)} + \frac{Z_g}{\alpha_g} \quad (11)$$

$\alpha(x)$ is the condensing heat transfer coefficient of the mixture calculated for pure component, Shahs' correlation, using the local physical properties of the mixture. The single phase heat transfer coefficient of the vapour α_g is calculated with the Dittus-Bolter correlation based on vapour properties. The parameter Z_g is the ratio of the sensible cooling of the vapour to the cooling rate.

$$Z_g = \chi\,\frac{\Delta T cp_g}{\Delta h} \quad (12)$$

Where X is the local vapour quality, cp_g is the specific heat of the vapour, ΔT is the temperature glide and Δh is the enthalpy change of the mixture. The total enthalpy change is that of the latent heat plus sensible heat. The latter can be estimated as the mean of the liquid and vapour specific heat, as follow:

$$\Delta h = \left(\frac{cp_g + cp_l}{2} \times \Delta T_{dew}\right) + h_{fg} \quad (13)$$

This method has been applied to hydrocarbon mixture and more recently to binary and ternary zeotropic blends, *Thome (2008) [11]*.

4. Air Side Heat Transfer Coefficient

4.1. Air Side Surface Efficiency

The fin performance is commonly expressed in terms of heat transfer coefficient and thermal fin efficiency. It is defined as the ratio of the actual fin heat transfer rate to the heat transfer rate that would exist if all the fin surfaces are at the base temperature, *Perrotin* and *Clodic (2003) [12]*. For enhanced fin geometry, louvered or slit fins, the present work uses the Schmidt's circular fin approximation analysis which overestimates the fin efficiency by up to (5%), *Stewart, (2003) [10]*. For plate fin, Schmidt (1945) suggested that the plate fin can be divided into hexagonal shape fin, as shown in Fig. 3. Then, he analyzed hexagonal fin and concluded that they can be treated as circular fin by replacing the outer radius of the fin with the equivalent radius. The empirical relation for the equivalent radius is given by:

$$\frac{r_e}{r_t} = 1.27\,\Psi(\beta - 0.3)^{\frac{1}{2}} \quad (14)$$

Where r_t is the outside radius. The coefficients Ψ and β are defined as:

$$\Psi=\frac{B}{r_t}$$

$$\beta=\frac{H}{B}$$

For the present analysis,
$B=X_l$ if $X_l < X_t/2$, otherwise $B=X_t/2$

$$H=\frac{1}{2}\sqrt{\left(\frac{X_t}{2}\right)^2+{X_l}^2}$$

After the evaluation of the equivalent radius, the equation for standard circular fin can be used. In this study, the length of fin is much greater than the thickness so the parameter (m) is defined as:

$$m=\left(\frac{2\alpha_a}{k_f\,t_f}\right)^{\frac{1}{2}} \tag{15}$$

The fin efficiency parameter can be defined as:

$$\Phi=\left(\frac{r_e}{r_t}-1\right)\left(1+0.35\ln\left(\frac{r_e}{r_t}\right)\right) \tag{16}$$

The fin efficiency can be defined as a function of (Φ, m, r_t)

$$\eta_f=\frac{\tanh(m\,r_t\,\Phi)}{m\,r_t\Phi} \tag{17}$$

The total surface efficiency is given by:

$$\eta_s=1-\frac{A_f}{A_o}(1-\eta_f) \tag{18}$$

The fin area and total area are given by:

$$A_f=\left[(W\times H)-\left(\frac{\pi}{4}\,D_o^2\right)\right]\times 2\times n_f \tag{19}$$

$$A_t=(\pi D_o L)-(\pi\,D_o\,n_f\,t_f) \tag{20}$$

$$A_o=A_f+A_t \tag{21}$$

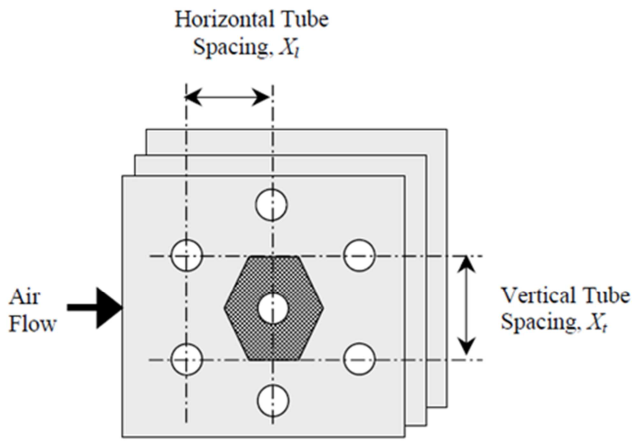

Figure 3. *Staggered Tube Configurations.*

4.2. Air Side Correlation

To calculate overall heat transfer coefficient, air side heat transfer coefficient must be known. For louvered fin Wang correlation, cited in *Stewart (2003) [10],* is applied to determine the Colburne j- factor which is associated with heat transfer coefficient by:

$$\overline{\alpha_a}=\frac{jC_pG_{max}}{Pr^{2/3}} \tag{22}$$

where $G_{max:}$ is the mass flux of the air through the minimum flow area $\left(\frac{\dot{m}_a}{A_{min}}\right)$.

The specific heat in the above equation is replaced by the humid specific heat, as suggested by *Tarrad et al. (2007) [13]* and *(2008) [14]* in which air conditioning range is taken as (1.022 $\frac{kJ}{kg.K}$). The Colburne j-factor values are listed in table 2.

Table 2. *The Colburne j- factor in (22).*

Re<1000	Re≥1000
$j=14.3117\,(Re_{Dc})^{J1}\left(\frac{F_s}{D_c}\right)^{J2}\left(\frac{L_h}{L_p}\right)^{J3}\left(\frac{F_s}{X_L}\right)^{J4}\left(\frac{X_L}{X_t}\right)^{-1.724}$	$j=1.1373\,(Re_{Dc})^{J5}\left(\frac{F_s}{X_L}\right)^{J6}\left(\frac{L_h}{L_p}\right)^{J7}\left(\frac{X_L}{X_t}\right)^{J8}Z^{0.3545}$
$J1=-0.991-0.1055\left(\frac{X_L}{X_t}\right)^{3.1}\ln\left(\frac{L_h}{L_p}\right)$	$J5=-0.6027+0.02593\left(\frac{X_L}{D_{h,w}}\right)^{0.52}Z^{-0.5}\ln\left(\frac{L_h}{L_p}\right)$
$J2=-0.7344+2.1059\left(\frac{Z^{0.55}}{\ln(Re_{Dc})-3.2}\right)$	$J6=-0.4776+0.40774\left(\frac{Z^{0.7}}{\ln(Re_{Dc})-4.4}\right)$
$J3=0.08485\left(\frac{X_L}{X_t}\right)^{-4.4}Z^{-0.68}$	$J7=-0.58655\left(\frac{F_s}{D_{h,w}}\right)^{2.3}\left(\frac{X_L}{X_t}\right)^{-1.6}Z^{-0.65}$
$J4=-0.1741\ln(Z)$	$J8=0.0814\,(\ln(Re_{Dc})-1)$

For the staggered tube arrangement, the minimum flow area is calculated using the relation cited in *Subbarao (2008) [15]*, as follows:

$$A_{min}=\left[\left(\left(\frac{L}{X_t}-1\right)C\right)+\left((X_t-D_o)\left(1-(t_f\times n_f)\right)\right)\right]H \tag{23}$$

In which C is such that:

$$C=2\times a\ \text{ if } 2\times a<2\times b$$

$$C=2\times b\ \text{ if } 2\times b<2\times a$$

here

$$2\times a=(X_t-D_o)\times(1-t_f\times n_f) \tag{24}$$

$$b=\left[0.5\times {X_t}^2\right]^{0.5}-D_o-(X_t-D_o)\times t_f\times n_f \tag{25}$$

where

$$D_{h,w}=\frac{4A_{min}}{L}$$

Re_{Dc} is the Reynolds number of air based on the collar diameter ($D_c=D_o+2t_f$).

The louver pitch (L_p) and high (L_h) are (2mm) and (1mm) respectively. The number of rows (Z) is used as one.

5. Refrigerant Side Pressure Drop

Pressure drop can be broken down into three components, gravitational, acceleration (momentum) and frictional pressure drop which represent the potential energy, kinetic energy of the fluid and that due to friction on the channel wall, so:

$$\Delta P_{total} = \Delta P_{static} + \Delta P_{momentum} + \Delta P_{friction} \quad (26)$$

For horizontal tube, there is no change in static head so $\Delta P_{static} = 0$. The pressure drop due to momentum and friction will be considered with distinction between two phase and single phase flow.

5.1. Single-phase Pressure Drop

Frictional pressure drop can be calculated using the fanning equation with the fanning friction factor, *Domanski and Didion (1983) [2],* as follows:

$$\Delta P = \frac{2\, f\, G^2 L}{D_i\, \rho} \quad (27)$$

$$f = 0.046\, R_e^{-0.2} \quad (28)$$

Pressure drop due to momentum change can be calculated, as follows:

$$\frac{dP}{dL} = -G^2 \frac{d\upsilon}{dL} \quad (29)$$

Here (G) is the refrigerant mass flux and (L) is the tube length.

5.2. Two-Phase Pressure Drop

For R-22 flow through the condenser, the momentum pressure drop is given by:

$$\Delta P_{mom} = \frac{16\dot{m}^2}{\pi^2 D^4}\left\{\left[\frac{\chi_o{}^2}{\rho_g \epsilon_o} + \frac{(1-\chi_o)^2}{\rho_l(1-\epsilon_o)}\right] - \left[\frac{\chi_i{}^2}{\rho_g \epsilon_i} + \frac{(1-\chi_i)^2}{\rho_l(1-\epsilon_i)}\right]\right\} \quad (30)$$

The void fraction ϵ, is defined as the vapour volume to the total volume and can be predicted by using Zivi (1964) cited in *Sweeney* and *Chato (1996) [16]*.

$$\epsilon = \frac{1}{1+\left(\frac{1-\chi}{\chi}\right)\left(\frac{\rho_g}{\rho_l}\right)^{0.67}} \quad (31)$$

For frictional pressure drop, one of the most accurate two-phase pressure drop correlations is used; this correlation is due to Friedel. It is used by optimizing an equation for ϕ_{fo}^2 using a large data base of two-phase pressure drop measurement, *Quiben (2005) [17]*. This model for vapour quality and utilizes a two-phase multiplier as:

$$\Delta P_{friction} = \Delta P_{Lo} \phi_{fo}^2 \quad (32)$$

$$\phi_{fo}^2 = E + \frac{3.24\, F\, H}{Fr_H^{0.045}\, We_L^{0.035}} \quad (33)$$

The Froude number Fr_h, E, F and H are:

$$Fr_h = \frac{G^2}{g D \rho_h^2} \quad (34)$$

$$E = (1-\chi)^2 + \chi^2 \frac{\rho_l f_{Go}}{\rho_g f_{Lo}} \quad (35)$$

$$f_{Lo} = \frac{0.079}{Re_{Lo}^{0.25}} \quad (36)$$

$$f_{Go} = \frac{0.079}{Re_{Go}^{0.25}} \quad (37)$$

$$F = \chi^{0.78}(1-\chi)^{0.224} \quad (38)$$

$$H = \left(\frac{\rho_l}{\rho_g}\right)^{0.91}\left(\frac{\mu_g}{\mu_l}\right)^{0.19}\left(1-\frac{\mu_g}{\mu_l}\right)^{0.7} \quad (39)$$

Liquid Weber number We_L is:

$$We_L = \frac{G^2\, D}{\sigma \rho_h} \quad (40)$$

The homogeneous density ρ_h is defined as:

$$\rho_h = \left(\frac{\chi}{\rho_g} + \frac{1-\chi}{\rho_l}\right)^{-1} \quad (41)$$

In the above correlation, the value of (χ) is considered to be a mean value between the entering and leaving sides of the tube in the form: $\chi = \frac{\chi_i + \chi_o}{2}$.

For R407C and R407A, the new correlation developed by *Choi et al. (1999) [18]* is used. This correlation was developed depending on a data base consisting of the following pure and mixed refrigerants: R125, R134a, R32, R410A, R22, R407C and R32/R134a (25/75% mass). This correlation predicted the measured micro-fin data with an average residual of (10.8%) and it also predicted the pressure drop in smooth tube with an average residual of (15%). The correlation was given in the form:

$$\Delta P = \Delta P_{friction} + \Delta P_{acceleration}$$

$$= \left\{\frac{f_N L(\upsilon_{out} - \upsilon_{in})}{D} + (\upsilon_{out} - \upsilon_{in})\right\} G^2 \quad (42)$$

Specific volumes of the two-phase fluid are obtained from a linear quality weighted sum of the vapour and liquid specific volumes at either the outlet or inlet of the tube. The new two-phase friction factor is:

$$f_N = 0.00506 R_{e_{fo}}^{-0.0951} K_f^{0.1554} \quad (43)$$

The friction factor is based on the liquid Reynolds number and the two-phase number, $K_f = \frac{\Delta X\, h_{fg}}{Lg}$ and (L) corresponds to the tube length.

6. Overall Heat Transfer Coefficient

By using the heat transfer coefficient of refrigerant and air with the inclusion of the surface fouling and fin effect [19], the overall heat transfer coefficient can be expressed as:

$$UA=\left\{\frac{1}{(\eta_s \alpha A)_r}+\frac{R''_{f,r}}{(\eta_s A)_r}+R_w+\frac{R''_{f,a}}{(\eta_s A)_a}+\frac{1}{(\eta_s \alpha A)_a}\right\}^{-1} \quad (44)$$

The conductance resistance (R_w) is obtained from $R_w=\frac{\ln(r_o/r_i)}{2\pi kL}$. The fouling factors are assumed to be (0.0004) $\left(\frac{m^2.K}{W}\right)$, (0.0002) $\left(\frac{m^2.K}{W}\right)$ and (0.0004) $\left(\frac{m^2.K}{W}\right)$ for refrigerant vapor, liquid and air respectively [20]. Since there are no fins on the refrigerant side of the tubes, the refrigerants side efficiency is (1).

7. Model Verification and Discussion

7.1. Model Prediction

The experimental results are compared to the theoretical simulation using *CONTBT (Condenser Tube by Tube)* program built in the present study. The results showed a good agreement with the implemented experimental data. The deviation of the predicted variables, heat duty and air dry bulb temperature, from the experimental data is defined as:

$$\Phi^{\mp}=(\Phi_{\text{theoretical}}-\Phi_{\text{experimental}})/\Phi_{\text{experimental}} \quad (45)$$

The predicted duty when circulates R22 or R407C refrigerants revealed under predicted behavior by (-5%) and (-4%) respectively as shown in Fig. 4. On the contrary, R407A simulation results exhibited almost over prediction up to (+1.7 %).

The value of theoretical air temperature predicted by the *CONTBT* program is taken as a mean value of all of the estimated values from the tube outlet at the fourth row. The maximum deviation estimated between the experimental tests and theoretical simulation is:

- When R22 refrigerant is used, the maximum discrepancy of the condenser inlet temperature ranges between (+21.3 % and – 7.8 %) occurring during (30°C) and (28°C) condenser inlet temperature respectively.
- When R407C refrigerant is circulated, the maximum discrepancy in air temperature simulation is (11.6% and -11%) for (38°C) and (36°C) condenser air temperature.
- When R407A is circulated, it was found that all of the data were over predicted, the maximum discrepancy was calculated to be (24.3%) for (30 °C) inlet condenser temperature.

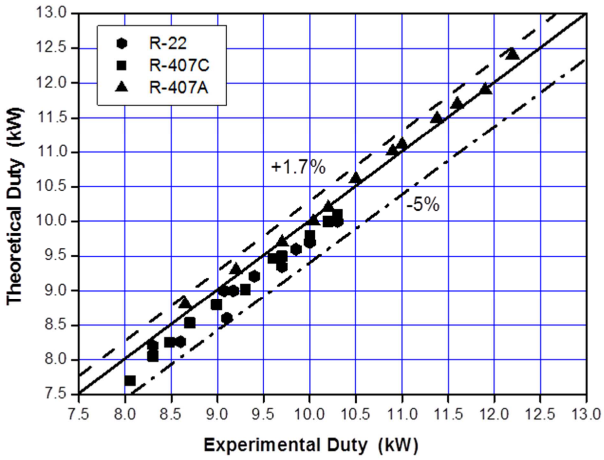

Figure 4. *Model Simulation of the Condenser Duty for the Test Refrigerants.*

7.2. Graphical Representation of Condenser Load Distribution

The superheated refrigerant enters the condenser at the first, second and third rows respectively and the exit of these rows are brought together by a header then the refrigerant enters the fourth row. Definitely, these circuits arrangement will put the owning shadow on the thermal performance of the condenser.

Fig. (5) shows the condenser load distribution for R22 and its candidate refrigerants. The simulation results for R22 refrigerant show that, the condenser load in the desuperheating zone reveals a mean value equal to (47.6 W), (46.8 W), (46.5 W) for row number one, two and three respectively.

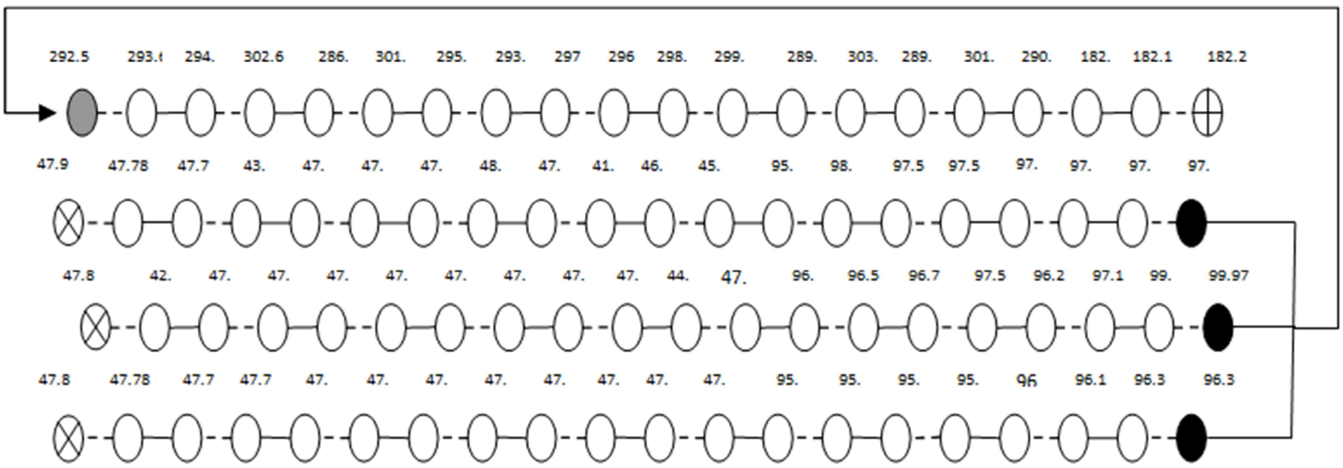

(a) Load distribution visual representation of R22.

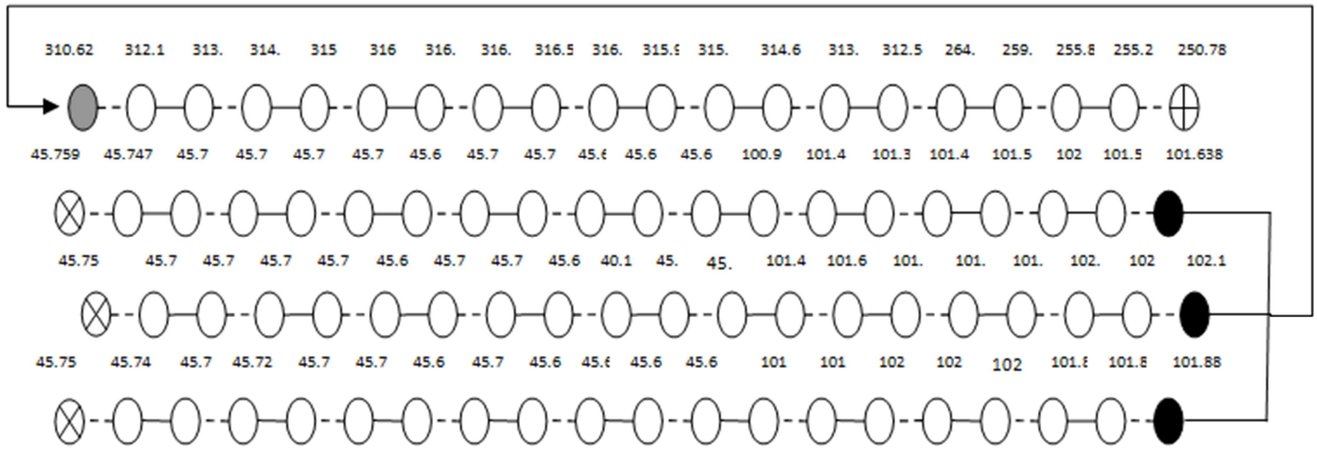

(b) Load distribution visual representation of R407C.

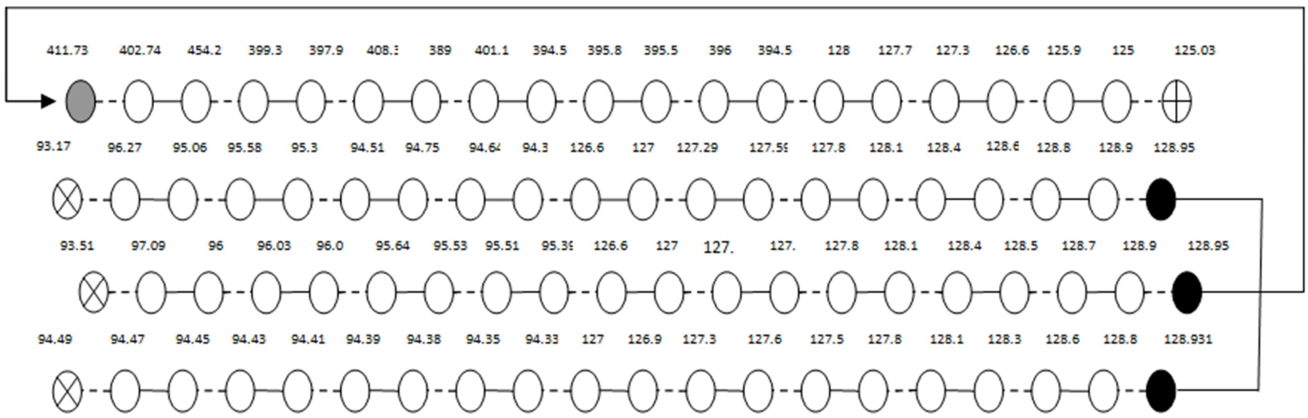

(c) Load distribution visual representation of R407A.

Figure 5. *Condenser Load Distribution for Simulated Data at T_{air}=36 ℃.*

At the two phase zone, the tube condenser duty will take almost (97 W) for the first three rows. As these rows merge together to compose the fourth row, the mass flow rate of the refrigerant will be three folds and hence the tube condenser load becomes triplicate. The remainder of the two phase zone occupies the fourth row have almost a value which ranges between (286-303 W). After the desuperheating and condensation zone has finished, the sub-cooled zone has begun. The results show that it exhibits almost constant value of (182 W), Fig. (5.a).

For R407C, the desuperheating zone simulation results show that the tube condenser duty possesses almost the mean value of (45.5 W) for the first three rows. In the condensation zone, the first three rows take almost a mean value of (101.6 W). The fourth row and referring to the same reason mentioned previously, then the tube condenser duty takes a value which ranges between (310-316.5 W), Fig. (5.b).

The same trend is observed when R407A is circulated in the RAC except that the numerical values are higher than those of the other refrigerants. However, the desuperheating zone rejected almost a tube condenser load equal to (94.9 W) for the first three rows, Fig. (5.c). It takes a mean value of (128 W) in the condensation zone.

On the other hand, the rest of the condensation zone that occupies the fourth row takes a value ranges between (389-454 W). In the sub-cooled zone the tube heat duty value ranges between (125-128W).

7.3. Graphical Representation of Entering Air Temperature Distribution

The backward technique is followed in CONTBT simulation program for the air side of the condenser. As shown in Fig. (6), the inlet air temperature is drawn past each tube. For R22 refrigerant, the exit measured temperature from the condenser is (55.3 ℃) and, the mean predicted values of the simulated inlet air temperature to 1st, 2nd, 3rd and 4th were (55.1, 50.2, 43, 38.5 ℃) respectively, Fig. (6.a). In addition, the measured inlet air temperature to the condenser was (36 ℃). So, the percentage deviation of the inlet air temperature to the condenser is (7%). The same trend was observed when the air temperature has been simulated for R407C and R407A. For R407C, the simulated inlet air temperature of the condenser is (37.4 ℃) which indicates that the percentage deviation is (4%); whereas, the simulated air temperature is (40.2℃) when R407A is used which indicates that the percentage deviation is (11.7%).

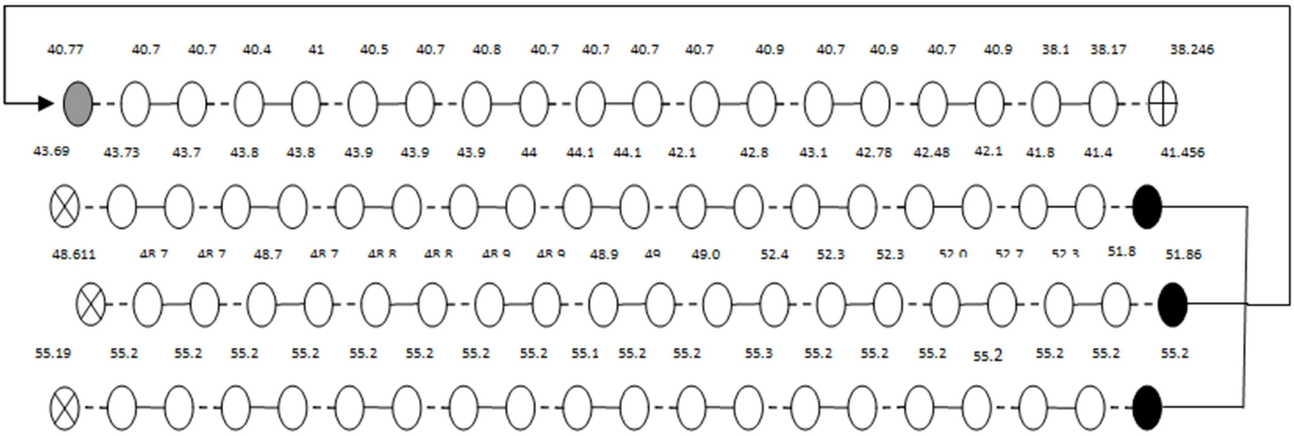

(a) Entering Air temperature visual representation of R22 results.

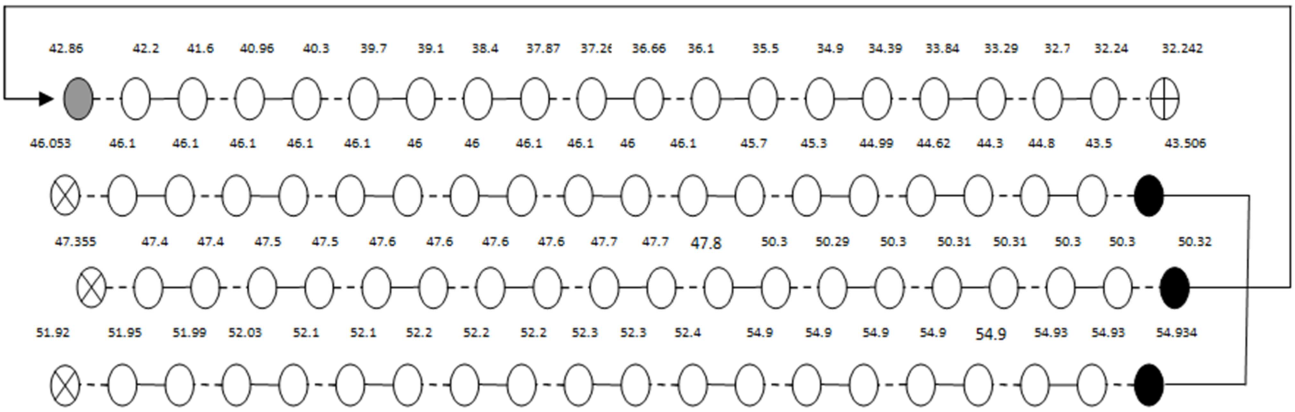

(b) Entering Air temperature visual representation of R407C results.

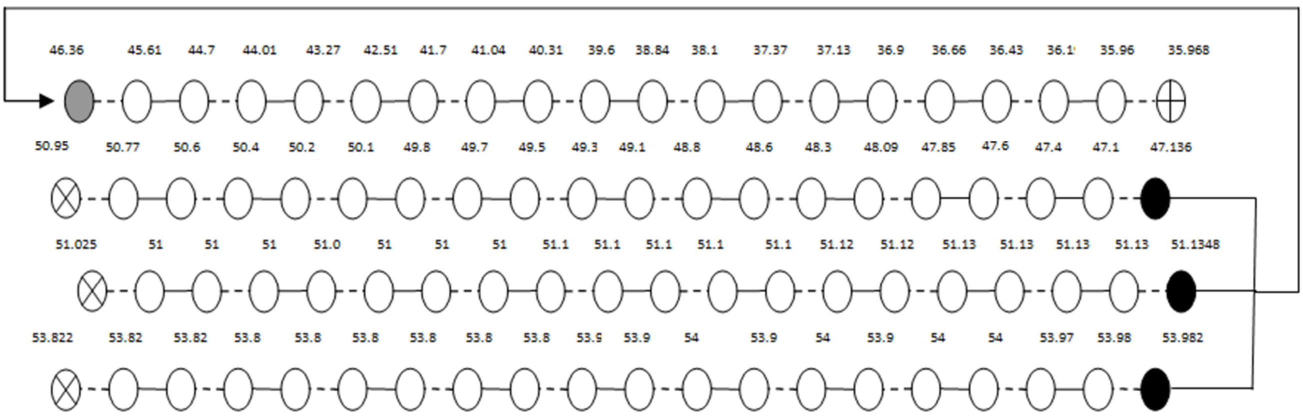

(c) Entering Air temperature visual representation of R407A results.

Figure 6. *Condenser Air Inlet Temperature Distribution for Simulated Data at T_{air}=36*°C.

8. Conclusions

The following represent the important outcomes from the present work:

1. It is considered to be a good addition to the work of refrigerant alternatives of halocarbons implemented in the manufacturing of refrigeration units.
2. It represents a practical thermal tool for the rating objectives of air cooled condensers regardless of the application target of these heat exchangers. It showed excellent agreement between the experimental and predicted data of the entering air dry bulb temperature and condensation load.

3. It is recommended to test the present rating model with other type of refrigerants for the validation purposes of refrigerant alternatives. This is to predict the performance of the cooling unit prior to get the decision of refrigerant substitutes.

Nomenclature

A: The total surface area or Cross sectional area (m^2).
cp: Specific heat (kJ/kg.K).
D: Tube diameter (m).
f: Friction factor, function.
Fr: Froude number (dimensionless).
Fs: Fin spacing (m).
g: Gravitational acceleration (m/s^2).
G: Mass flux ($\frac{kg}{m^2.s}$).
h: Enthalpy (kJ/kg).
h_{fg}: Latent heat (kJ/kg).
H: Height of heat exchanger (m) or parameter defined elsewhere.
j: Colburne j-factor.
k: Thermal conductivity ($\frac{W}{m.K}$).
K_f: Two-phase number.
L: Flow length (Depth of the coil) (m).
L_h: Louver height (m).
L_p: Louver pitch (m).
$\dot{m}$: Mass flow rate (kg/s).
n_f: Number of fin.
Nu: Nusselt number (dimensionless).
P: Pressure (Mpa).
P_r: Reduced pressure (P/P_c).
Pr: Prandle number (dimensionless).
$\dot{Q}$:Heat load(W).
r_e: Equivalent radius (m).
r_t: Outside tube radius (m).
Re: Reynolds number (dimensionless).
Re_{Dc}: Reynolds number of the air based on collar diameter.
R'': Fouling factor (m^2. K/W).
R_w: Wall resistance (K/W).
St: Stanton number (dimensionless).
t: time (sec).
t_f: Fin thickness (m).
U: Overall heat transfer coefficient (W/m^2. K).
V: Velocity (m/s).
W: Width of heat exchanger (m).
W_a: Humidity ratio (kg of steam/kg of dry air).
$\dot{W}$: Work (kW).
We: Weber number (dimensionless).
X: Mass fraction (quality) (dimensionless), concentration.
X_l: Longitudinal (horizontal) tube spacing (m).
X_t: Transverse (vertical) tube spacing (m).
z: Elevation (m).
Z: Number of row.
Z_g: Ratio of the sensible cooling of the vapor to the cooling rate.

Subscript

a: Air.
D: Diameter of the tube.
Dc: Collar diameter.
Di: Inner diameter.
e: Equivalent.
f, a: fouling air.
f, r: Fouling refrigerant.
f: Fin.
fg: Denotes the difference between saturated vapor and saturated liquid at the same property.
fo: Fluid only.
g: gas, vapor.
Go: Gas only.
h: Homogenous, high.
l: Liquid.
Lo: Liquid only.
nb: nucleate pool boiling contribution.
o: Total or outside value.
r: reduced.
s: Surface.
t: Tube.
tf: Two-phase.
v: vapor.

Greek Symbols

$\bar{\propto}$: A single phase heat transfer coefficient ($\frac{W}{m^2.K}$).
ϕ_{fo}^2: Two-phase multiplier.
$\Phi^{\mp}$: Percentage deviation (%).
Δh: Enthalpy change of the mixture.
ΔT: Temperature glide (℃), Temperature difference.
$\propto$: Heat transfer coefficient ($\frac{W}{m^2.K}$).
ϵ: Void fraction (dimensionless).
η: Efficiency.
μ: Viscosity ($\frac{kg}{m.s}$).
ρ: Density ($\frac{kg}{m^3}$).
υ: Specific volume ($\frac{m^3}{kg}$).
σ: Surface tension ($\frac{N}{m}$).

References

[1] Ellison, R. D., Creswick, F. A., Fisher, S. K., and Jackson, W. L.," A Computer Model for Air-Cooled Refrigerant Condensers with Specified Refrigerant Circuiting", ASHRAE Transaction, Vol. 87, Oak Ridge National Laboratory (ORNL), Oak Ridge, Tennessee, 1981.

[2] Domanski, P. A., and Didion, D. A., " Computer Modeling of the Vapour Compression Cycle with Constant Flow Area Expansion Device", Center of Building Technology, National Bureau of Standards, Washington, USA, May, 1983.

[3] Kempiak, M. J. and Crawford, F. R.," Three-Zone Modeling of a Mobile Air Conditioning Condenser", Air Conditioning and Refrigerating Center (ACRC), University of Illinois, Mechanical Industrial Engineering Department, Urbane, April, 1991.

[4] Bensafi, A. and Borg, S., "Design and Simulation of finned-Tube Heat Exchanger Using Pure and Mixed Refrigerants", Belgium, Proceedings of Clima 2000 conference, held in Burssels, August 30th to September 2nd 1997.

[5] Sadler, E. M., "Design Analysis of a Finned-Tube Condenser for a Residential Air Conditioner using R22", M. sc thesis, The Academic Faculty, Georgia Institute of Technology, April 2000.

[6] Wright, M. F., "Plate-Fin-and Tube Condenser Performance and Design for Refrigerant R410A Air-Conditioner", M. sc thesis, The Academic Faculty, Georgia Institute of Technology, May 2000.

[7] Tarrad, A. H. and Khudor, D. S., "A Correlation for the Air Side Heat Transfer Coefficient Assessment in Continuous Flat Plate Finned Heat Exchangers", Transactions of the ASME, Journal of Thermal Science and Application, Vol. (7), No. 2, Paper No. TSEA-14-1194, DOI: 10.11151/1.4029459, 2015.

[8] Tarrad, A. H. and Altameemi, A. F., "Experimental and Numerical Model for Thermal Design of Air Cooled Condenser", Global Journal of Researches in Engineering (GJRE-A), Mechanical and Mechanics Engineering, Volume 15, Issue 3, Version 1.0, pp. 11-26, 2015.

[9] Al-Nadawi, A. K., "Experimental and Theoretical Study of R407C and R407A as Alternatives of R22 Refrigerant in a Window Type Air Conditioner", MSc. Thesis, Mechanical Engineering Department, College of Engineering, Al-Mustansiriya University, 2010.

[10] Stewart, S. W., "Enhanced Finned - Tube Condenser Design and Optimization", PhD thesis, The Academic Faculty, Georgia Institute of Technology, November, 2003.

[11] Thome, J. R., "Engineering Data Book III", Faculty of Engineering Science and Technology, Swiss Federal Institute of Technology Laussanne (EPEL), Switzerland, Wolverine Tube, INC, 2008.

[12] Perrotin, T. and Clodic, D.," Fin Efficiency Calculation in Enhanced Fin-And-Tube Heat Exchangers in Dry Conditions", International Congress of Refrigeration, Washington, USA, pp. 1-8, 2003.

[13] Tarrad, A. H. and Shehhab, U. S.," The Prediction of Environment Effect on the Performance of a Vapour Compression Refrigeration System in Air Conditioning Application", Journal of Engineering and Development. Vol. 11, No. 1, pp. 169-189, March 2007.

[14] Tarrad, A. H., Khudor D. S., and Abdul Wahed M., "A simplified Model for the Prediction of the Thermal Performance for Cross Flow Air Cooled Heat Exchangers with a New Air Side Thermal Correlation", Engineering and Development Journal, Vol. 12, No. 3, September 2008.

[15] Subbarao, P. M., "Fin- Tube Condenser and Evaporator with Delta Winglet Window A/C", Mechanical Engineering Department, Indian Institute of Technology, Delhi, iitd. ac. in., 2008.

[16] Sweeney, K. A. and Chato, J. C., "The Heat Transfer and Pressure Drop Behavior of a Zeotropic Refrigerant Mixture in a Micro-Finned Tube", Air Conditioning and Refrigerating Center (ACRC), University of Illinois, Mechanical Industrial Engineering Department, Urbane, May, 1996.

[17] Quiben, J. M., "Experimental and Analytical Study of Two-Phase Pressure Drops during Evaporation in Horizontal Tubes", PhD thesis, DEA-Dynamique des Fluides et des Transferts, Universite, Pierre et Mari Carie, Paris, France, Laussanne, 2005.

[18] Choi, J. Y., Kedzierski, M. A., and Domanski, P. A., "A Generalized Pressure Drop Correlation for Evaporation and Condensation of Alternative Refrigerants in Smooth and Micro-Fin Tubes", National Institute of Standards and Technology (NIST), Gaithersburg, USA, October 1999.

[19] Incropera F. P. and DeWitt D. P., 1985. "Fundamentals of Heat and Mass Transfer", 2nd edition, John Wiley & Sons Inc., USA.

[20] Janna W. S., 2000. Engineering Heat Transfer, 2nd edition, CRC press LLc, USA.